Pressure-induced semimetallic behavior of calcium from *ab initio* calculations

M V Magnitskaya[1], N L Matsko[2], V S Baturin[2] and Yu A Uspenskii[2]

[1] L.F. Vereshchagin Institute for High Pressure Physics, Russian Academy of Sciences, 142190 Troitsk, Moscow, Russia
[2] P.N. Lebedev Physical Institute, Russian Academy of Sciences, Leninskii prosp. 53, 119991 Moscow, Russia

E-mail: magnma@gmail.com

Abstract. A loss of metallic properties in fcc calcium under high pressure is studied *ab initio* using the density functional theory (DFT) and *GW* approximation. It is found that a more correct description of many-electron effects given by *GW* method does not provide significant changes in the behavior of electronic spectrum in comparison with DFT approach. We note that the obtained width of (pseudo)gap is highly sensitive to the **k**-point sampling used for density of states calculation. The analysis of fcc calcium's band structure at $p \sim 20$ GPa shows that the crossing of bands at the Fermi level is removed if the spin-orbit coupling is taken into account.

1. Introduction

Pressure-induced partial 'dielectrization' of electronic spectrum in the fcc phase of alkaline-earth metals Ca and Sr, as well as similar to them (isovalent and isostructural) rare-earth metal Yb, has long attracted attention of both experimental and theoretical physicists (see, e.g., review paper [1]). Experimentally, upon compression the electrical resistance ρ of the three elements noticeably increases and reaches a maximum at a certain pressure value (not exceeding 15 GPa), the effect being most pronounced in case of Yb [2–4]. In addition, near this pressure value, a thermopower anomaly is observed for each of these elements [4–6]. Upon further compression, the re-entrance of metallic resistivity occurs at the point of structural transition to a bcc phase that remains metallic at all pressures. Notice that this pressure-induced transition occurs from a close-packed to more loosely-packed structure, in contrast, say, to alkali metals, where the opposite structural sequence is observed.

Of the three divalent elements mentioned, Ca exhibits the weakest resistance anomaly. Its resistance begins to increase at $p \sim 5$–6 GPa and reaches maximum values between the pressures of 12 and 19.5 GPa [3], the latter corresponds to the fcc→bcc transition [7]. In this pressure range, calcium behaves as a semimetal or narrow-band semiconductor, with a negative temperature coefficient of resistance from 77 to 300 K [3].

There are many *ab initio* calculations of band structure and phase transformations in Ca, however, only some of them [1, 8–13] touch upon the loss of metallicity in the fcc phase. Notice that each of these studies on Ca predicts different onset pressures for semimetallic behavior, which are, in turn, in rather poor agreement with experiment. The spread in values is rather wide — 4 to 19 GPa for metal–semimetal and 7 to 21 GPa for semimetal–metal transitions. In early publications [8–10], much attention has been paid to the choice of approximation for exchange and correlation. However, these

efforts did not eliminate uncertainties concerning the pressure range where a semimetallic state of Ca occurs. It is also not completely clear, whether a real gap or a pseudogap exists in this pressure range. The situation looks more definite for Sr and Yb, where the energy gap, small as it is, has apparently been obtained in *ab initio* calculations [14–16].

In this paper, we report on electronic structure calculations of Ca in the range of stability of the fcc phase — from normal pressure p = 1 atm to 20 GPa. The aim of this work is to find out the origin of (pseudo)gap and understand what parameters of calculation determine the pressure range of semimetallic behavior in Ca.

2. Calculation method

Our calculations were mainly performed in the framework of density functional theory (DFT) [17], with semilocal generalized gradient approximation (GGA) for exchange-correlation potential [18]. We employed the Vienna Ab-Initio Simulation Package (VASP) [19] and the projector augmented wave (PAW) pseudopotential method [20]. The Brillouin zone (BZ) was sampled with Monkhorst–Pack **k**-point meshes [21] and the valence electron configuration $3s^2p^64s^2$ was taken. The integration over BZ was carried out using the improved tetrahedron method [22]. The maximum number of **k**-points in the 1/48 irreducible BZ used for evaluating the electron density of states was equal to 3107 (the 50×50×50 sampling). The plane wave cutoff of 280 eV was chosen, which gives the total energy convergence of 10^{-6} eV. To adequately explore fine details of electronic spectra, the spin-orbit coupling was taken into account.

The DFT approach precisely describes crystal structures and total energies. The Kohn–Sham eigenvalues provide sufficiently accurate approximation for quasiparticle electronic spectra for most metals [17]. However, as is well known, the energy gaps are underestimated within DFT, which is related to the use of local exchange-correlation potentials. For this reason, we also employed the *GW* method [23], in which the quasiparticle spectra are obtained from the Dyson equation using the following simple approximation to the self-energy operator:

$$\Sigma^{GW}(\mathbf{r},\mathbf{r}',E)=\frac{\mathrm{i}}{2\pi}\int \mathrm{d}E' G(\mathbf{r},\mathbf{r}',E+E')W(\mathbf{r},\mathbf{r}',E') \quad . \tag{1}$$

Here, $G(\mathbf{r}, \mathbf{r}', E + E')$ is the single-electron Green function and $W(\mathbf{r}, \mathbf{r}', E')$ is the dynamically screened Coulomb interaction. The combination of two symbols G and W that appear in Eq. (1) is used as the method name. The *GW* method provides the dielectric gaps and entire quasiparticle spectra of solids in good agreement with experiment. The main shortcoming of this method is high computational cost, about 1000 times higher compared to DFT, which is due to exact calculation of $W(\mathbf{r}, \mathbf{r}', E')$. The self-energy Σ^{GW} is non-local and energy dependent, which provides a more precise description of quasiparticle spectra.

As fully converged *GW* calculations are exceedingly demanding, we used the so-called G_0W_0 approximation which is known to be sufficiently accurate [24]. In this approximation, the DFT-GGA eigenvalues and eigenfunctions are used to construct a first guess to the Green function, G_0, and screened Coulomb interaction, W_0. Then the Dyson equation is solved with the self-energy $\Sigma^{G_0W_0}$. Thus, actually only the first iteration is done. Our test runs made up to the fourth iteration, G_4W_4, provided the results not too different from those obtained with G_0W_0 approximation. The *GW* calculations were made with the following parameters: maximum 145 **k**-points in the IBZ (the 16×16×16 grid), 96 bands involved in self-energy calculation, the energy cutoff of about 190 eV, and frequency grid spacing of 0.45 eV.

3. Results and discussion

Electronic structure of Ca was computed at several compressions $\xi = V/V_0$, where V and V_0 are specific volumes at given pressure p and normal pressure p_0, respectively. A value of pressure corresponding to a particular relative volume V/V_0 can be determined from the $T = 0$ equation of state, $p(V)$, measured

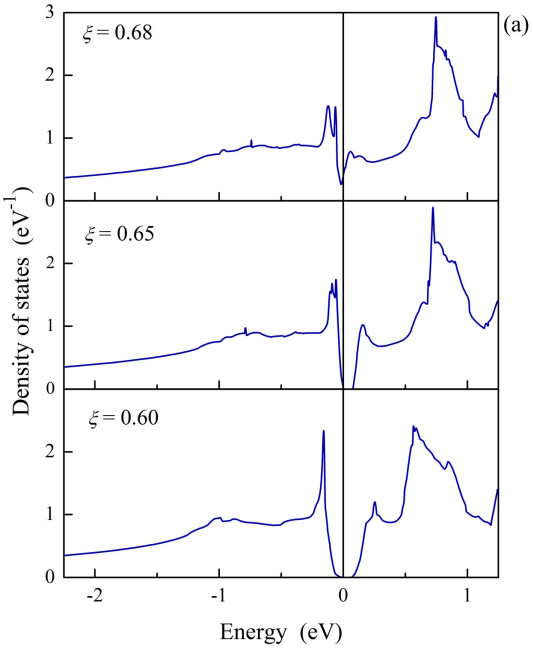

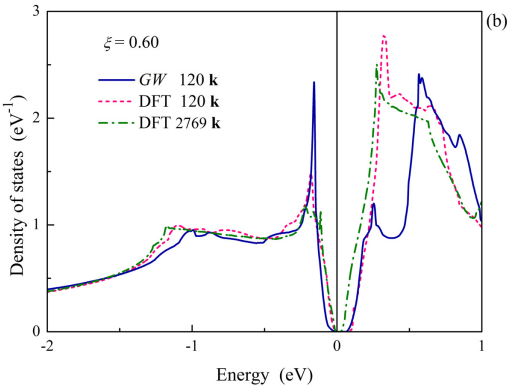

Figure 1. Density of states of fcc Ca at various relative volumes $\xi = V/V_0$; 120 **k**-points in the IBZ, Fermi level is set to zero. (a) *GW* calculations, pressure increases from top to bottom. (b) Comparison of DOS at $\xi = 0.6$ in different approximations: *GW* (full line), DFT (dots), DFT, 2769 **k**-points (dash-dotted line).

experimentally or calculated from first principles. The obtained VASP results well agree with our previous calculations [1] performed using the all-electron Augmented Plane Wave (APW) method. Hence, to evaluate the pressure, we used the equation of state obtained in [1]. The highest considered compression was $0.6V_0$, which corresponds to $p \sim 20$ GPa.

A non-zero density of states (DOS) at the Fermi level, $D(E_F)$, is a characteristic of metal. The DOS of fcc Ca calculated within *GW* approximation at three volumes is drawn in Figure 1a. On compression, $D(E_F)$ decreases and at $V/V_0 \sim 0.67$ becomes equal to zero. Upon further compression, $D(E_F)$ remains zero down to $0.6V_0$, where the bcc phase becomes energetically preferable over the fcc phase. As is seen, the gap width increases with pressure. In our DFT calculations made with the same grid of 120 **k**-points, a compression at which $D(E_F)$ vanishes is somewhat lower ($\sim 0.72V_0$). That is the change of exchange-correlation interaction somehow affects the electronic spectrum.

Figure 1b shows the comparison of DOS at $V/V_0 \sim 0.6$ for *GW* (full line) and DFT (dotted line) calculations. It is seen in the figure that there is a significant distinction between the two DOS curves in the conduction band region, while the valence band remains almost unaffected. The energy gap width also does not noticeably change as the *GW* approximation is applied.

These *GW* results are most probably not fully converged with respect to **k**-point sampling. However, increasing the **k**-point number $N_{\mathbf{k}}$ in *GW* calculations is computationally very expensive. The DFT calculations are far less demanding, so we made several test computations with considerably denser **k**-grids up to 3107 **k**-points in the IBZ. These tests demonstrate that with progressively increasing $N_{\mathbf{k}}$, the gap width is reduced and the pressure of metal-to-semimetal transition increases. The DOS for 2769 **k**-points is displayed in Figure 1b, together with the *GW* and DFT results for 120 **k**-points. The DOS profiles for 2769 (dash-dotted line) and 120 **k**-points (dotted line) are similar to each other. The main difference is that in the former case, the gap width is five times larger. As is seen, the **k**-point number $N_{\mathbf{k}}$ is more important for the gap width than the choice of approximation for exchange and correlation. Notice that the pressure of gap occurrence also significantly depends on this number.

The reason for such sensitivity of the gap width to the $N_{\mathbf{k}}$ value can be illustrated in the corresponding band structure plots. The results of our VASP calculations are presented in Figure 2, where the comparison of calcium's band structure at normal volume V_0 (a) and $V = 0.6V_0$ (b) is shown.

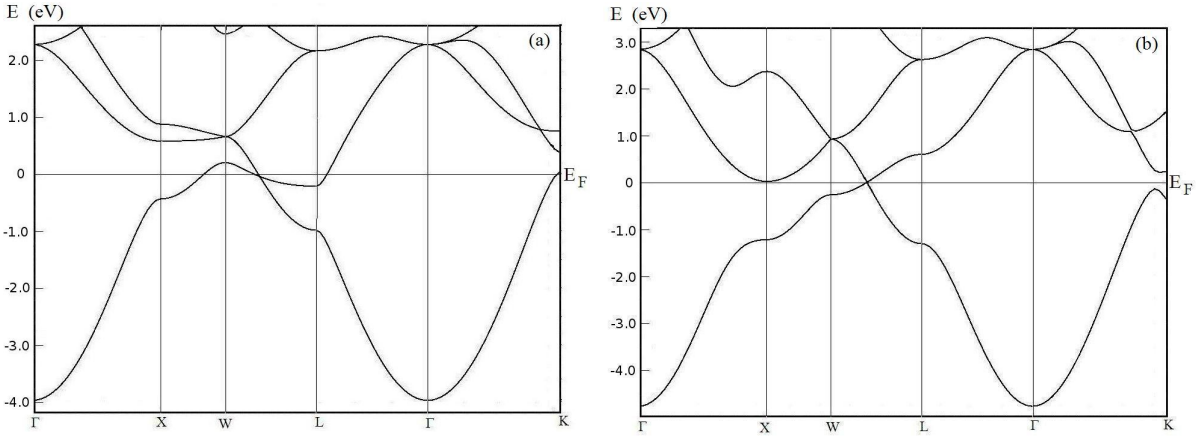

Figure 2. Band structure of fcc Ca along high-symmetry directions of BZ at normal volume V_0, $p \approx 0$ (a) and on compression to $V = 0.6V_0$, $p \sim 20$ GPa (b).

It is seen in the figure that the only place where the bands intersect the Fermi level E_F, is the point of crossing (accidental degeneracy) between the first and the second bands in the W–L line of BZ. That is, the $p = 0$ Fermi surface of Ca consisting of equal-sized hole and electron parts, almost disappears at $V/V_0 = 0.6$, which corresponds to a semimetallic state. Similar behavior of band structure upon compression has been found in other calculations of Ca [8–10], as well as Sr and Yb [14–16].

The existence of band crossing in the W–L line implies that the DOS at E_F is very small but not zero. The origin of the gap seen in the DOS plots (Figure 1) is related to the way how the DOS is constructed by the corresponding algorithm. Namely, for any index i, the ith band at the point $\mathbf{k}_1$ is connected with the ith band at the neighbouring point $\mathbf{k}_2$. Band intersections are determined by compatibility relations for the symmetry groups of adjacent **k**-vectors. However, the procedure of DOS calculation does not support the analysis of wave function symmetry at all **k**-vectors, which is actually not important for DOS evaluation. Thus, the dependence of gap width on **k**-point number $N_\mathbf{k}$ is related to the accuracy of describing the band crossing. The larger $N_\mathbf{k}$, the narrower is the gap. Strictly speaking, the spectra shown in Figure 1 are characterized by a pseudogap with extremely low DOS values around the Fermi level. This picture is qualitatively the same within both DFT and *GW* approaches, so in *GW* calculations, one should also expect the gap narrowing with increasing $N_\mathbf{k}$. However we did not check this directly because of high computational cost involved.

It is natural to suppose that the existence of semimetallic (or semiconducting) state in fcc divalent metals can be due to the fact that the accidental degeneracy of the two lowest bands in W–L line is lifted by spin-orbit (SO) coupling. According to the relativistic *ab initio* calculations [14, 15] of heavier elements Sr and Yb (atomic numbers $Z = 38$ and 70), the SO coupling does remove the degeneracy in the W–L direction. A maximum SO splitting Δ_{SO} of bands found for Sr and Yb is of ~0.1 and ~0.3 eV, respectively [14, 15]. For calcium with $Z = 20$, one should expect a several times smaller value of SO splitting (~0.02 eV), because $\Delta_{SO} \sim 1/Z^2$.

In paper [12] the effect of SO interaction on electronic structure of Ca has been considered using an assumed value of SO coupling constant. The paper's authors, however, refrain from exact estimates based on the fact the SO interaction for Ca is very weak. We performed relativistic PAW calculations of fcc Ca at $V = 0.6V_0$ on the mesh of 3107 **k**-points. It turned out that for the SO splitting to be reliably evaluated, a high **k**-space resolution corresponding to 400 points along the W–L direction is necessary. It should be noted that the calculation [12] of Ca band structure was made on the mesh of 89 **k**-points in the IBZ, with a larger number of 505 **k**-points used for DOS integration. Probably, it is a rather coarse **k**-point sampling that did not allow for exploring the effect of SO coupling in [12].

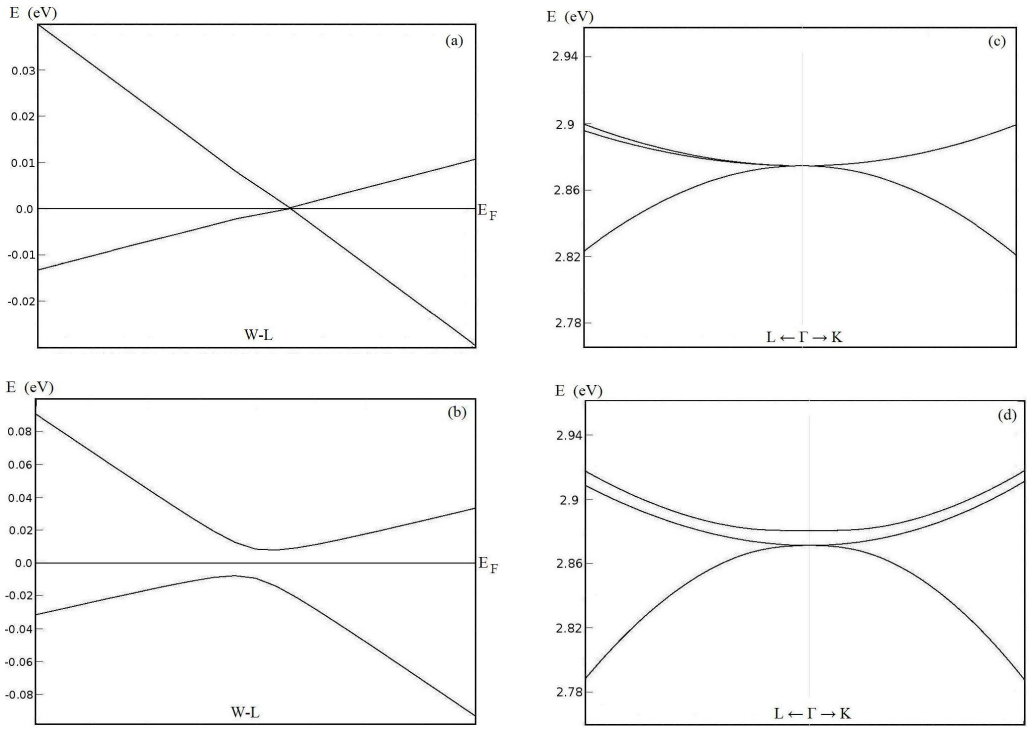

Figure 3. Band structure of fcc Ca at $V = 0.6V_0$ on an enlarged scale. (a, b) the first and the second bands in the W–L direction evaluated without and with SO coupling, respectively. (c, d) the triply degenerate $\Gamma_{25'}$ level at the Γ point, without and with SO coupling, respectively. Energy is measured from the Fermi level E_F.

An enlarged view of the vicinity of E_F along the W–L line calculated without and with SO coupling is shown in Figures 3a and 3b, respectively. As is seen, the SO coupling in Ca, small as it is, definitely removes the degeneracy of two lowest bands at the Fermi level E_F. For reference, the neighborhood of a triply degenerate $\Gamma_{25'}$ level is also presented, with and without SO coupling (Figure 3d and 3c, respectively). The threefold degeneracy of $\Gamma_{25'}$ level is seen to be lifted by SO interaction according to symmetry relations. The obtained value of SO splitting Δ_{SO} ~0.01 eV for the $\Gamma_{25'}$ level and ~0.015 eV for the levels near the crossing point. These values are close to the above estimate. It follows from the fcc lattice symmetry that the $\Gamma_{25'}$ level at the Γ point is d-like (t_{2g}), while the two lowest bands in the W–L line that belongs to the hexagonal face of BZ are largely p-like. As is known, the higher orbital quantum number l, the less the amplitude of corresponding wave function near the core region, which mainly contributes to SO interaction. Therefore, it is only natural that SO splitting Δ_{SO} for $\Gamma_{25'}$ level is less than for the p-like levels in Figure 3b.

4. Conclusions

To conclude, we studied from first principles the changes that occur in the electronic properties of fcc Ca on compression down to the relative volume $V/V_0 = 0.6$ ($p \sim 20$ GPa). An analysis of factors and calculation parameters expected to influence the results was made. Our DFT calculations were made using the semilocal gradient approximation for the exchange-correlation potential. The electronic spectrum of Ca near $0.6V_0$ is observed to exhibit a pseudogap feature due to the crossing (accidental degeneracy) of two lowest bands at the Fermi level E_F. Application of the more exact non-local *GW* approximation significantly changes the conduction band shape, but hardly affects the valence band and pseudogap region, as compared to our DFT results.

The description of the pseudogap region is shown to be much more sensitive to the **k**-point number $N_{\mathbf{k}}$ used for DOS evaluation than to the choice of approximation for exchange and correlation. This is not surprising, because the larger $N_{\mathbf{k}}$, the more accurate is the description of the mentioned band crossing at E_F. In our DFT–GGA calculations, the **k**-point number was gradually increased up to 3107 **k**-points in the IBZ, while the *GW* calculations, because of their high computational cost, were made with considerably smaller $N_{\mathbf{k}}$. For the same reason, we investigated the effect of spin-orbit coupling also only within DFT. In this case the accidental degeneracy of bands is lifted, which gives rise to a rather small band splitting of 0.015 eV at the band crossing point. In principle, it is of interest to carry out similar GW calculations with increasing k-point number and SO coupling included, but in our opinion, this would not qualitatively change the obtained DFT results.

The calculated value of SO splitting is close to the limit of computational accuracy. Nevertheless such narrow gaps could affect the low-frequency response, and thereby be observable in optical experiments in the IR region. The described behavior of calcium's electronic spectrum upon compression should manifest itself in the pressure dependence of dc electrical resistivity, especially if one bears in mind that the application of high pressure produces numerous defects in a solid, with accompanying energy states within the gap. Notice that our calculations are performed at zero temperature. At room temperature, the existence of these states, with their number unknown, may lead to some discrepancies in behavior between a real material and perfect crystal. Anyway, the small energy gap should be thermally smeared out, because its estimated width is of the order of 100 K. In our opinion, it is this smeared gap which is responsible for the weak resistivity and thermopower anomalies experimentally observed in Ca at high pressure and room temperature.

Acknowledgements
The authors acknowledge funding from Russian Academy of Sciences, Russian Foundation for Basic Research (Nos. 12-02-31638, 12-02-31774, 13-02-00655 and 13-02-00913) and the Government of Russian Federation (No. 14.A12.31.0003). The numerical calculations are performed at the Joint Supercomputer Center of RAS.

References

[1] Maksimov E G, Magnitskaya M V and Fortov V E 2005 Non-simple behavior of simple metals at high pressure *Phys. Usp.* **48** 761–80
[2] McWhan D B, Rice T M and Schmidt P H 1969 *Phys. Rev.* **177** 1063–71
[3] Dunn K J and Bundy F P 1981 *Phys. Rev.* B **24** 1643–50
[4] Divakar C, Mohan M and Singh A K 1982 *Solid State Commun.* **41** 833–4
[5] Chandra Shekar N V, Meng J F, Polvani D A and Badding J V 2000 *Solid State Commun.* **116** 443–5
[6] Brazhkin V V, Tsiok O B and Magnitskaya M V 2013 *JETP Lett.* **97** 490–4
[7] Olijnyk H and Holzapfel W B 1984 *Phys. Lett.* A **100** 191–4
[8] Altmann S L, Harford A R and Blake R G 1971 *J. Phys.* F: *Metal Phys*. **1** 791–805
[9] McCaffrey J W, Anderson J R and Papaconstantopoulos D A 1973 *Phys. Rev*. B **7** 674–84
[10] Mickish D J, Kunz A B and Pantelides S T 1974 *Phys. Rev.* B **10** 1369–83
[11] Jan J P and Skriver H L 1981 *J. Phys.* F: *Metal Phys*. **11** 805
[12] Wang G M, Papaconstantopoulos D A and Blaisten-Barojas E 2003 *J. Phys. Chem. Solids* **64** 185
[13] Oganov A R, Ma Y, Xu Y, Errea I, Bergara A and Lyakhov A O 2010 *PNAS* **107**, 7646–51
[14] Johansen G and Mackintosh A R 1970 *Solid State Commun*. **8** 121–4
[15] Kubo Y 1987 *J. Phys.* F: *Metal Phys*. **17** 383
[16] Mutlu R H 1996 *Phys. Rev.* B **54** 16321–4
[17] Hohenberg P and Kohn W 1964 *Phys. Rev*. **136** B864
Kohn W and Sham L J 1965 *Phys. Rev*. **140** A1133
[18] Perdew J P, Burke K and Ernzerhof M 1996 *Phys. Rev. Lett.* **77** 3865

[19] Kresse G and Furthmüller J 1996 *Comp. Mater. Sci.* **6** 15–50
[20] Blöchl P E 1994 *Phys. Rev.* B **50** 17953–79
[21] Monkhorst H J and Pack J D 1979 *Phys. Rev.* B **13** 5188–92
[22] Blöchl P E, Jepsen O and Andersen O K 1994 *Phys. Rev.* B **49** 16223–33
[23] Hedin L and Lundqvist S 1970 Effects of electron-electron and electron-phonon interactions on the one-electron states of solids *Solid State Physics* (vol. 23) ed F Seitz, D Turnbull and H Ehrenreich (New York: Academic) pp 1–181
[24] Aryasetiawan F and Gunnarson O 1998 *Rep. Prog. Phys*. **61** 237